Progress In Electromagnetics Research B, Vol. 10, 21–34, 2008

PARALLEL FLOW VELOCITY SHEAR KELVIN HELMHOLTZ INSTABILITY WITH AC ELECTRIC FIELD

R. S. Pandey and U. C. Srivastava

Department of Applied Physics
Amity School of Engineering and Technology
Amity University
Noida-125 UP, India

S. Kumari

Department of Physics
Vinoba Bhave University
Hazaribag, India

A. Kumar

Department of Physics
SPM College
Udantpuri, Biharsharif, India

Abstract—Electrostatic velocity shear Kelvin-Helmholtz instability has been studied for bi-Maxwellian plasma in the presence of perpendicular a.c. electric field by using the method of characteristic solution. The effects of a.c. electric field temperature variation, velocity shear scale length, electron ion temperature ratio and other parameters on growth rate have been discussed.

1. INTRODUCTION

The Kelvin-Helmholtz instability is generated by unbalanced pressure resulting from the perturbation of the velocity shear flow. The Kelvin-Helmholtz (K-H) instability that is driven by sheared velocity flows has applications in many areas of astrophysics and space physics. In the beginning of the space era Axford and Hines [1] have suggested that the solar wind couples momentum and energy into the magnetospheric

cavity via a viscous interaction along the flanks of the day side magnetopause. They speculated that the strong velocity shear at the boundary might excite Kelvin-Helmholtz turbulence, which would then permit solar wind momentum to diffuse in the closed magnetospheric field lines. This viscous stress would drive a tail ward convection flow, which eventually would be closed by an earth ward return flow in the center of the tail.

When the flow is perpendicular to the ambient field, shear flow occurs due to a nonuniform electric field. Ganguli et al. [2–4] show that such a situation also gives rise to instabilities. Electrostatic particle simulation has also been employed to reveal more fully the character of the instability in the ion cyclotron regime [5, 6]. Pritchett and Coroniti [7, 8] have carried out similar simulation for the longer wavelength electrostatic Kelvin Helmholtz instability, showing reduction of growth when the ion gyroradius becomes comparable to the shear layer thickness. In recent parallel flow velocity shear instabilities has been studied with inhomogeneous D.C. electric field for an anisotropic Maxellian plasma [9, 10]. While attempts have been made to study such ion kinetic instabilities by including in the MHD formulation first-order finite Larmor radius corrections [7] or Proton and electron pressure effects [11] the modifications to the MHD theory are minimal. Recently, Opp and Hassan [12] have used a set of modified MHD equations, which are valid in the large Larmor radius limit, to show that a new short wavelength branch of the Kelvin-Helmhoitz instability is also excited [13].

Simulation of K-H instability for magnetospheric applications are numerous [14, 15]. In order to study K-H mixing process, the ion particle effects have been treated consistently in hybrid code simulation including the effect of inhomogeneity in density [16]. The motivation for this work is provide by observations of both space and laboratory plasmas in which flows have been reported, whose shear scale length can be of the order of the ion Larmor radius or smaller. In auroral phenomena, for example electric fields called paired electrostatic shocks have been found to exist whose scale length of variation is of the order of the ion Larmor radius [17, 18]. This electric field causes localized cross-field flows, which excite instability with frequency and growth rate in the vicinity of the ion cyclotron frequency [2, 3]. A distinctive feature of this instability is that it can exist even when the field-aligned current is sub critical. Another example of strongly sheared system is given by the dynamical evolution of the plasma sheet just prior to the on set of a magnetic substrom. During this time the neutral plasma sheet region thins and its width becomes smaller than the ion Larmor radius.

In this paper electrostatic K-H instability for short wave length has been studied with perpendicular AC electric field for bi-Maxwellian plasma by using the method of characteristic solution in auroral region of ionosphere. The effect of a.c. electric field temperature variation, density gradient and other parameters has been discussed. The bi Maxwellian modified distribution including density gradient and velocity shears has been used in this study. The most important source of driving instability is velocity shear, temperature anisotropy, density gradient and AC frequency, which modify the Doppler shift frequency.

2. DISPERSION RELATION

A spatially homogeneous anisotropic magnetoplasmacollision less magneto plasma subjected to an external magnetic field $B_0 = B_0 e' z$ and an electric fields $E_{0x} = (E_0 \sin \upsilon t e' x)$ has been considered. In order to obtain the dispersion relation in this case, the Vlasov-Maxwell equations are linearized. The linearized equations obtained after neglecting the higher order terms and separating the equilibrium and non equilibrium parts, following the techniques of [9, 19] are given as

$$\upsilon \frac{\delta f_{s0}}{\delta r} + \frac{e_s}{m_s} \left[E_o \sin \upsilon t + (v \times B_o) \right] \left(\frac{\delta f_{so}}{\delta v} \right) = 0 \tag{1}$$

$$\frac{\delta f_{s1}}{\delta t} + v \cdot \frac{\delta f_{s1}}{\delta r} + \left(\frac{F}{m_s} \right) \left(\frac{\delta f_{s1}}{\delta v} \right) = S(r, v, t) \tag{2}$$

where force is defined as $F = mdv/dt$, υ = a.c. frequency

$$F = e_s \left[E_0 \sin \upsilon t + (v \times B_0) \right] \tag{3}$$

The practical trajectories are obtained by solving the equation of motion defined in Eq. (3) and $S(r, v, t)$ is defined as

$$S(r, v, t) = \frac{-e_s}{m_s} \left[E_1 + (v \times B_1) \right] \left(\frac{\delta f_{so}}{\delta v} \right) \tag{4}$$

where s denotes species and E_1, B_1 and f_{s1} are perturbed and are assumed to have harmonic dependence in f_{s1}, B_1 and $E_1 \sim \exp i(k \cdot r - \omega t)$.

The method of characteristic solution is used to determine the perturbed distribution function. f_{s1}, which is obtained from Eq. (2) by

$$f_{s1}(r, v, t) = \int_{\circ 0^\circ}^{\infty} S \left\{ r_o \left(r, v, t' \right), v_0 \left(r, v, t' \right), t - t' \right\} dt' \tag{5}$$

The phase space coordinate system has been transformed from (r, v, t) to $(r_0, v_0, t - t')$. The particle trajectories which have been obtained by solving Eq. (3) for the given external field configuration and wave propagation

$$k = \lfloor k_\perp e_x, 0, k_\parallel e_z \rfloor.$$

are

$$\begin{aligned}
X_0 &= X + \left(\frac{v_y}{\Omega_{cs}}\right) + \left(\frac{1}{\Omega_{cs}}\right)\left[v_x \cos\Omega_{cs}t' - v_y \cos\Omega_{cs}t'\right] \\
&\quad + \left(\frac{\Gamma_x}{\Omega_{cs}}\right)\left[\frac{\Omega_{cs}\sin\upsilon t' - \upsilon \sin\Omega_{cs}t'}{\Omega_{cs}^2 - \upsilon^2}\right] \\
Y_0 &= y + \left(\frac{v_x}{\Omega_{cs}}\right) - \left(\frac{1}{\Omega_{cs}}\right)\left[v_x \cos\Omega_{cs}t' - v_y \sin\Omega_{cs}t'\right] \\
&\quad - \left(\frac{\Gamma_x}{\upsilon\omega_{cs}}\right)\left[\frac{\upsilon^2 \cos\Omega_{cs}t' - \Omega_{cs}^2 \cos\upsilon t'}{\Omega_{cs}^2 - \upsilon^2}\right] \\
Z_0 &= Z - v_z t'
\end{aligned} \tag{6}$$

and the velocities are

$$\begin{aligned}
v_{x0} &= v_x \cos\Omega_{cs}t' - v_y \sin\Omega_{cs}t' + \left\{\frac{\nu\Gamma_x(\cos\upsilon c' - \cos\Omega_{cs}t')}{\Omega_{cs}^2 - \upsilon^2}\right\} \\
v_{y0} &= v_x \sin\Omega_{cs}t' + v_y \cos\Omega_{cs}t' - \left\{\frac{\Gamma_x(\Omega_{cs}\sin\upsilon t' - \upsilon\sin\Omega_{cs}t')}{\Omega_{cs}^2 - \upsilon^2}\right\} \\
v_{z0} &= v_z
\end{aligned} \tag{7}$$

where $\Omega_{cs} = \frac{e_s B_0}{m_s}$ is the cyclotron frequency of species s and $\Gamma_x = \frac{e_s E_0}{m_s}$.

Equation (2) can be written in terms of a perturbed quantities as

$$\begin{aligned}
S\left(r_o, v_o, t - t'\right) \;=\; &-\left(\frac{e_s}{m_s\Omega}\right) e^{i\{kr_0(r,v,t) - \Omega(t - t')\}} \\
&+ \left[\left(\Omega - k \cdot v_o\right) E_1 + \left(v_0 \cdot E_1\right) k\right]\left(\frac{\delta f_{s0}}{\delta v}\right)
\end{aligned} \tag{8}$$

The unperturbed distribution function with velocity and density

gradient.

$$\begin{aligned} f_{s0} &= f_{m0} + V_y\varepsilon'' \\ \varepsilon'' &= \frac{1}{\Omega_s}\left[\frac{2\left(v_\parallel v_{ox}(x)\right)}{\alpha_{\parallel s}^2}\frac{dv_{ox}(x)}{dx}\right] f_{m0} \\ f_{m0} &= \frac{n_0}{\pi 3/2\alpha_{\perp s}^2\alpha_{\parallel s}^2}\exp\left[-\frac{\left(v_{ox}^2+v_{oy}^2\right)}{\alpha_{\perp s}^2}-\frac{\left(v_\parallel - v_{oz}(x)\right)^2}{\alpha_{\parallel s}^2}\right] \end{aligned} \quad (9)$$

where ε'' being constant of motion

$$\alpha_{\perp\parallel s}^2 = \frac{\left(2K_B T_\perp, T_\parallel, s\right)}{m_s}$$

After using the unperturbed trajectories with perpendicular AC electric field and unperturbed distribution function also doing some lengthy simplifications the perturbed distribution function as,

$$\begin{aligned} f_{s1}(r,v,t) = & \frac{ie_s}{m_s\omega}\sum_{m,n,p,g} j_n(\lambda_1)J_m(\lambda_1)J_p(\lambda_2)J_g(\lambda_3)e^{(m-n)(\pi/2+\theta)}e^{i(g-p)(\pi/2+\theta)} \\ & \times[E_{1x}U^* + V^*E_{1y} + W^*E_{1z}]\times\frac{1}{\omega - k_\parallel v_\parallel - n\Omega_c - g\Omega_c + p\upsilon} \end{aligned} \quad (10)$$

where

$$\begin{aligned} U^* &= C_1\left(v_\perp\frac{n}{\lambda_1}+\frac{\upsilon\Gamma_x}{\Omega_c^2-\upsilon^2}\left(\frac{P}{\lambda_2}-\frac{n}{\lambda_1}\right)\right) \\ V^* &= iC_1\left(v\frac{J_n}{J_n}+\frac{\Gamma_x}{\Omega_c^2-\upsilon^2}\left(\Omega_c\frac{J_p}{J_p}-v\frac{n}{\lambda_1}\right)\right) \\ &\quad +\varepsilon''\left(1-K_\perp V_\perp\frac{n}{\lambda_1}-K_\perp\Omega\frac{\upsilon\Gamma_x}{\Omega_c^2-\upsilon^2}\left(\frac{p}{\lambda_2}-\frac{n}{\lambda_1}\right)\right) \\ W* &= DK_\perp V_\perp\frac{n}{\lambda_1}+\Omega\frac{\partial f_{si}}{\partial v_\parallel}+DK_\perp\frac{\upsilon\Gamma_x}{\Omega_c^2-\upsilon^2}\left(\frac{p}{\lambda_2}-\frac{n}{\lambda_1}\right) \\ C_1 &= \left(\omega - K_\parallel v_\parallel\right)\left(\frac{-2f_{so}}{\alpha_{\perp s}^2}\right)+k_\parallel\frac{\partial f_{so}}{\partial v_\parallel} \\ D &= \left(v_\parallel\left(\frac{-2f_{so}}{\alpha_{\perp s}^2}\right)-\frac{\partial f_{so}}{\partial v_\parallel}\right) \end{aligned}$$

$$\lambda_1 = \frac{k_\perp v_\perp}{\Omega_s}$$
$$\lambda_2 = \frac{k_\perp \Gamma_x}{\Omega_{cs}^2 - \upsilon^2}$$
$$\lambda_3 = \frac{v k_\perp \Gamma_x}{\Omega_c^2 - \upsilon^2}$$

Now simplifying $m = n$, $g = p$ and using the definition of current density, conductivity and dielectric tensor, we get the dielectric tensor

$$\varepsilon\left(k_1\omega\right) = 1 - \frac{4\pi c_s^2}{m_s\omega^2}\int \frac{d^3v\Sigma J_p\left(\lambda_2\right) J_g\left(\lambda_3\right)\left\|S_{ij}\right\|}{\omega - n\Omega_s - g\Omega_s + k_\| v_\| + p\upsilon} \tag{11}$$

where

$$S_{ij} = \begin{vmatrix} J_n^2 U^* \frac{n}{\lambda_1} v_\perp & J_n^2 V^* \frac{n}{\lambda_1} v_\perp & J_n^2 U^* \frac{n}{\lambda_1} v_\perp \\ -iJ_n J_n^{'} U^* V_\perp & -iJ_n J_n^{'} V^* V_\perp & -iJ_n J_n^{'} W^* V_\perp \\ J_n^2 U^* V_\| & J_n^2 V^* V_\| & J_n^2 W^* V_\| \end{vmatrix}$$

now we consider electrostatic instability

$$\|\varepsilon\| = N^2 \tag{12}$$

where $N =$ refractive index.

The required electrostatic dispersion relation can be obtained by using the technique of [9, 19] and from Eqs. (1) to (3)

$$\begin{aligned} D(k,\omega) = 1 + \frac{2\omega_{ps}^2}{k_\perp^2 \alpha_{\perp s}^2}\Gamma_n(\mu_s)\sum J_p(\lambda_2) J_g(\lambda_3)\eta_s \frac{k_\perp}{k_\|} \\ \times\left[\left\{\frac{\overline{\omega}}{k_\| \alpha_{\| s}} - \frac{1}{2}\varepsilon_n \rho_s \frac{\alpha_{\perp s}}{\alpha_{\| s}}\right\} Z(\xi_s)\right. \\ \left. - A_s \frac{\alpha_{\perp s}^2}{\alpha_{\| s}^2}(1 + \xi_s Z(\xi_s)) + A_T \frac{k_\|}{k_\perp}(1 + \xi_s Z(\xi_s)\right] \end{aligned} \tag{13}$$

where $Z(\xi)$ is plasma dispersion function,

$$\xi = \frac{\varpi - (n+g)\,\Omega_s + p\upsilon}{k_{||}\alpha_{\| s}}, \quad \eta_s = \left[1 - \frac{v\Gamma_{xs}}{\alpha_{\perp s}\left(\Omega_s^2 - v^2\right)} + \frac{vp}{n\Omega_s}\right],$$

$$A_s = \frac{1}{\Omega_s}\frac{dv_{oz}(x)}{dx}, \qquad A_T = \frac{\alpha_{\perp s}^2}{\alpha_{\parallel s}^2} - 1$$

$$\varepsilon_n = \frac{\delta l_n n(x)}{\delta x}, \qquad \varpi = \omega - k_\parallel v_{oz}(x)$$

$$\mu_s = \frac{k_\perp^2 P_s^2}{2}, \qquad \lambda_{Ds}^2 = \frac{\alpha_{\perp s}^2}{2\omega_p^2}$$

ω_p^2 = Plasma frequency, $\Gamma_n(\mu_s)$ = Modified Bessel Function.

Following the assumption of [21] and [9] for $p = 1$, $g = 0$ and $s = i, e$. In order to get dispersion relation for electrons and ions, approximations for electrons are assumed as $k_\perp \rho_e << 1$ and for ions no such assumptions in done thus above equations becomes.

$$D(k,\omega) = 1 + \frac{1}{k_\perp^2 \lambda_{Ds}^2}\eta_e \frac{T_{\perp e}}{T_{\parallel e}} + \frac{1}{k_\perp^2 \lambda_{Di}^2}\eta_i \left\{ \frac{T_{\perp i}}{T_{\parallel i}}\Gamma_n(\mu_i)\frac{k_\perp}{k_\parallel} \left\{ \left(\frac{\omega}{k_\parallel \alpha_{\parallel i}}\frac{T_{\perp i}}{T_{\parallel i}} - \frac{1}{2}\varepsilon_n \rho_i \frac{\alpha_{\perp i}}{\alpha_{\parallel i}} - \frac{n\Omega_i + p\upsilon}{k_\parallel \alpha_{\parallel i}} A_T \right) Z(\xi) - A_i \frac{T_{\perp i}}{T_{\parallel i}}(1 + \xi_i Z(\xi)) \right\} \right\} \tag{14}$$

After substituting $z(\varepsilon_i) = -\frac{1}{\varepsilon_i} - \frac{1}{2\varepsilon^3}$, $n_{oi} = n_{oe}$ and multiplying throughout by $\frac{k_\perp^2 \lambda_{Di}^2}{\eta i}$

$$\begin{aligned} 0 = {} & \frac{\lambda_{Di}^2 \eta_e T_{\perp e}}{\lambda_{De}^2 \eta_i T_{\parallel e}} + \left\{ \frac{T_{\perp i}}{T_{\parallel i}} - \Gamma_n(\mu_i)\frac{T_{\perp i}}{T_{\parallel i}} + \frac{\Gamma_n(\mu_i) k_\perp \varepsilon_n \rho_i \alpha_{\perp i}}{2 k_\parallel \alpha_{\parallel i}} \right. \\ & \times \frac{k_\parallel \alpha_{\parallel i}}{\varpi - n\Omega_i + p\upsilon} - \frac{\Gamma_n(\mu_i) k_\perp}{k_\parallel} \times \frac{k_\parallel \alpha_{\parallel i} + n\Omega_i}{\varpi - n\Omega_i + p\upsilon} \\ & \left. - \frac{\Gamma_n(\mu_i)}{2(\varpi - n\Omega_i + p\upsilon)^2} \frac{T_{\perp i}}{T_{\parallel i}} (k_\parallel \alpha_{\parallel i})^2 \left(1 - \frac{k_\perp}{k_\parallel} A_i\right) \right\} \end{aligned} \tag{15}$$

where

$$\eta_i = \left(1 - \frac{\upsilon \Gamma_{xi}}{\alpha_{\perp i}^2 (\Omega_i^2 - \upsilon^2)} + \frac{\upsilon p}{n\Omega_i}\right)$$

$$\eta_e = \left(1 - \frac{\upsilon \Gamma_{xe}}{\alpha_{\perp e}^2 (\Omega_e^2 - \upsilon^2)} + \frac{\upsilon p}{n\Omega_e}\right)$$

Multiplying throughout in Eq. (15) by $(\frac{\overline{\omega} - n\Omega_i + p\upsilon}{k_\parallel \alpha_{\parallel i}})^2$ we obtain a

quadratic dispersion as:

$$a_i \left(\frac{\varpi'}{\Omega_i}\right)^2 + b_i \left(\frac{\varpi'}{\Omega_i}\right) + c_1 = 0, \tag{16}$$

where

$$\begin{aligned}
a_1 &= a_2 \left(\frac{\Omega_i}{k_\parallel \alpha_{\parallel i}}\right)^2 \\
a_2 &= \frac{T_{\perp i}}{T_{\parallel e}}\frac{\eta_e}{\eta_i} + \frac{T_{\perp i}}{T_{\parallel i}} - \Gamma_n(\mu_i)\frac{T_{\perp i}}{T_{\parallel i}} \\
b_1 &= \frac{\Omega_i}{k_\parallel \alpha_{\parallel i}} b_2 - \frac{2p\upsilon}{\left(k_\parallel \alpha_{\parallel i}\right)^2} a_2 \Omega_i \\
b_2 &= \frac{k_\perp \Gamma_n(\mu_i)\varepsilon_n \rho_i \alpha_{\perp i}}{2k_\parallel \alpha_{\parallel i}} - \frac{k_\perp \Gamma_n(\mu_i)}{k_\perp} - \frac{k_\perp \Gamma_n(\mu_i) n\Omega_i}{k_{||}^2 \alpha_{\parallel i}} \\
c_1 &= \frac{\Gamma_n(\mu_i) T_{\perp i}}{2T_{\parallel i}} \left(1 - \frac{k_\perp}{k_\parallel} + A_i\right) - \frac{b_2 p\upsilon}{k_\parallel \alpha_{\parallel i}} + \frac{k_\perp^2 \upsilon^2 p^2}{\left(k_\parallel \alpha_{\parallel i}\right)^2} a_2 \\
\varpi' &= \varpi - n\Omega_i
\end{aligned}$$

The solution of Eq. (16) is

$$\varpi' = \frac{-b_i}{2a_i}\left[1 \pm \left(1 - \frac{4a_1 c_1}{b_1^2}\right)^{1/2}\right] \tag{17}$$

From this expression dimensionless growth rate has been calculated by computer technique when $b_i^2 < 4a_i c_i$. Hence this criteria gives a condition for the growth rate of wave when

$$A_i > \frac{k_\parallel}{k_\perp}\left[1 - \frac{2T_{\parallel i}}{\Gamma_0(\mu_i) T_{\perp i}}\left[\frac{\left(\frac{b_2\Omega_i}{k_\parallel \alpha_{\parallel i}} - \frac{2k_\perp p\upsilon \Omega_i a_2}{k_\parallel^2 \alpha_{\parallel i}^2}\right)^2}{4a_2\left(\frac{\Omega_i}{k_\parallel \alpha_{\parallel i}}\right)^2} + \frac{b_2 p\upsilon}{k_\parallel \alpha_{\parallel i}} - \frac{p_2 \upsilon^2 a_2}{k_\parallel^2 \alpha_{\parallel i}^2}\right]\right] \tag{18}$$

3. RESULTS AND DISCUSSION

Following plasma parameters suited to the ionospheric region have been used to evaluated the growth rate for harmonic value of $n = 0$.

Magnetic field B_0 has been taken to vary from 2×10^{-7} T to 6×10^{-7} T, energy of the electrons $K_BT_{\|} = 10\,\text{eV}$. Velocity shear scale length A_i has been allowed to vary between 0.5 to 0.6, density gradient $\varepsilon_n\rho_i$ between 0.02 to 0.06 and temperature ratio T_e/T_i between 2 to 4. The value of AC electric field has been fixed on $E_0 = 4\times10^{-3}\,\text{V/m}$ where as it's frequency ν is allowed to vary between 2 KHz and 4 KHz. Temperature anisotropy varies between 0.25 and 0.5 and the value of θ varies from 88° to 88.5° where $\theta = \tan -1\ (k_{\perp}/k_{\|})$. Growth rate variations with $k_{\|}\rho_i$ have been calculated from expression (17) for various values of plasma parameters listed in figure captions.

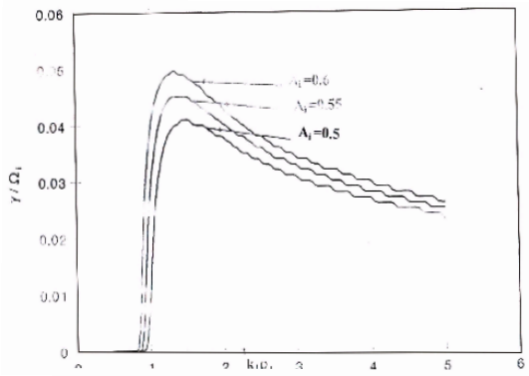

Figure 1. Variation of growth rate with $k_{\perp}\rho_I$ for various values of velocity shear scale length at other fixed plasma parameters.

Figure 1: The growth rate variations for two shear scale length have been shown. The maximum peak of growth rate is obtained at $k_{\perp}\rho_i = 1.4$ and and 1.5 respectively. The growth rate increases by increasing the velocity shear scale length but maxima shifts slightly towards higher value of $k_{\perp}\rho_i$. The mechanism of instability of this mode is de to coupling of regions of positive and negative wave energy. This coupling occurs if velocity shear is non-uniform and the shear is the source of energy. Figure 2 deals with variation of growth rate with $k_{\perp}\rho_i$ for different values of $\tan\theta = k_{\perp}/k_{\|}$ for maximum value of $k_{\perp}\rho_i = 1.5$. The growth rate increases by increasing the value of theta from 88° to 88.5° and maxima shifts towards higher value of $k_{\perp}\rho_i$. However, for some other plasma parameters and velocity shear, instability exists at lower angles with smaller magnitude. The K-H instability has maximum growth rate when c becomes very close to 90°.

Figure 3: It is shown that the magnetic field affects the growth rate. It increases by increasing the value of B_0 and maxima slightly

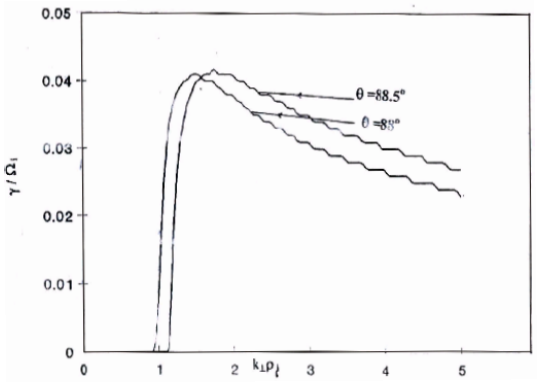

Figure 2. Variation of growth rate with $k_\perp \rho_I$ for various values of θ at other fixed plasma parameters.

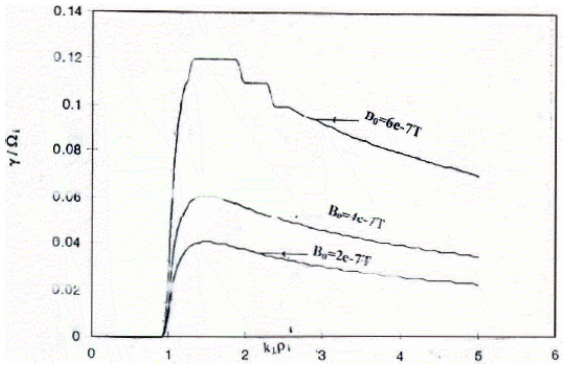

Figure 3. Variation of growth rate with $k_\perp \rho_I$ for various values of magnetic field B_0 at other fixed plasma parameters.

shifts towards higher values of $k_\parallel \rho_i$. Inhomogenity in magnetic field introduces a shear in velocity flow and couples positive and negative energy waves leading to grow of the wave. In Fig. 4, it clears that the growth rate is affected by the ratio T_e/T_i. It is increases by increasing the value of Te/Ti and maxima shifts towards higher value of $k_\perp \rho_i$ as the velocity shear term is proportional to T_e/T_i Thus , the temperature ratio of electron and ions becomes an additional source along with the velocity shear for exciting the larger wavelengths. When shear flow is dominated by electron flow, the maxima flows towards lower wavelengths [22].

Figure 5: The temperature anisotropy affects the growth rates

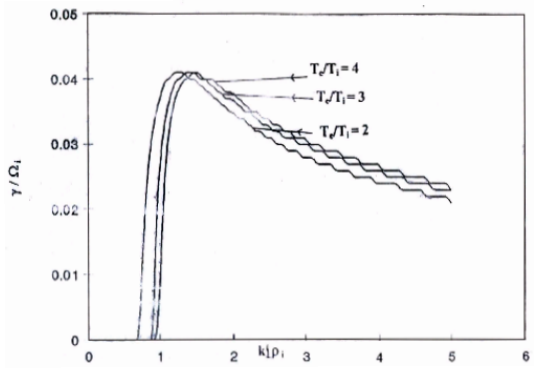

Figure 4. Variation of growth rate with $k_\perp \rho_I$ for various values of temperature ratio T_e/T_i at other fixed plasma parameters.

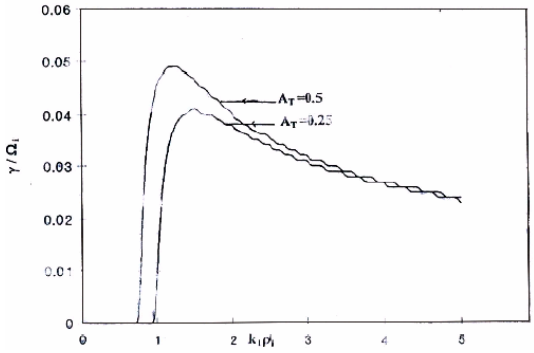

Figure 5. Variation of growth rate with $k_\perp \rho_I$ for various values of temperature anisotropy A_T at other fixed plasma parameters.

significantly and shifts towards lower value of $k_\perp \rho_i$. Tor towards the higher wavelengths. The non-isothermal plasma changes the velocity shear required for onset of this instability. Thus temperature anisotropy and electron ion temperature play a vital role in the understanding of magnetopause. Fig. 6 the variation of growth rate with $k_\perp \rho_i$ for various values of density gradient scale length from $\varepsilon_n \rho_i = 0.02$ to 0.06 the growth rate increases by the value ofv density scale length. The simulation conclusion of Fijimoto and Terasawa [16] indicates that for non-uniform background plasma, the mixing efficiency becomes the function of density ratio,shear width and wavelength of growing mode. The present analytical results are in agreement with their [16] conclusions. As shown in Fig. 7 the growth

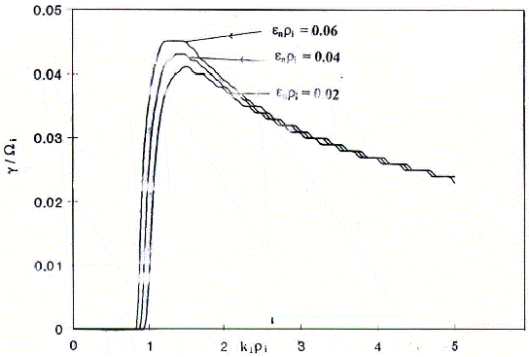

Figure 6. Variation of growth rate with $k_\perp \rho_I$ for various values of density gradient scale length at other fixed plasma parameters.

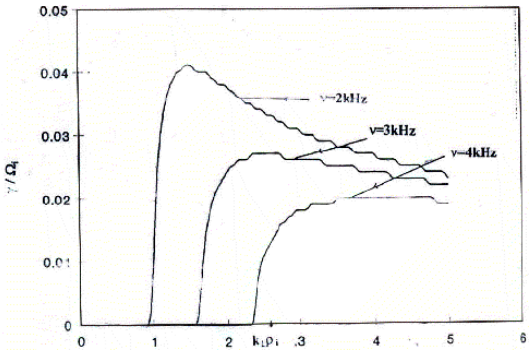

Figure 7. Variation of growth rate with $k_\perp \rho_I$ for various values of frequency of A.C. at other fixed plasma parameters.

rate increases by increasing the value of the frequency of the AC field and maxima shifted towards the higher values of $k_\perp \rho_i$. Indicate that the a.c. frequency modified the Doppler frequency.

4. SUMMARY

The prime driving source of K-H instability remains to be the velocity shear in addition temperature anisotropy and density gradient. The a.c. field frequency, which modifies the Doppler shift frequency having mark effect on K-H instability. The increasing in magnetic field plays the role of increasing effect of the growth rate. The electron ion ratio and pitch angle having minimum effect on this instability. The temperature anisotropy and a.c. frequency is worked as free energy

source for instability. The present results are in agreement with simulation results.

REFERENCES

1. Axford, W. I. and C. O. Hines, "A unifying theory of high latitude geophysical phenomena and geomagnetic storms," *Can. J. Phys.*, Vol. 39, 1433, 1961.
2. Ganguli, G., Y. C. Lee, and P. J. Palmadesso, "Electrostatic ion-cyclotron instability caused by a non-uniform electric field perpendicular to external magnetic field," *Phys. Fluids*, Vol. 28, 761, 1985.
3. Ganguli, G., Y. C. Lee, and P. J. Palmadesso, "Electron-ion hybrid mode due to transverse velocity shear," *Phys. Fluids*, 3D, 156, 1985.
4. Ganguli, G., Y. C. Lee, and P. J. Palmadesso, "Kinetic theory of electrostatic waves due to transverse velocity shears," *Phys. Fluids*, Vol. 31, 823, 1988.
5. Nishikawa, K. I., G. Ganguli, Y. C. Lee, and P. J. Palmadesso, "Simulation of ion-cyclotron like modes in a magnetoplasma with transverse imhomogeneous electric field," *Phys. Fluids*, Vol. 31, 1568, 1988.
6. Nishikawa, K. I., G. Ganguli, C. Lee, and P. J. Palmadesso, "Simulation of electrostatic turbulence due to sheared flows parallel and transverse to the magnetic field," *J. Geophys. Res.*, Vol. 95, 1029, 1990.
7. Pritchett, P. L. and F. V. Coroniti, "The collisionless macroscopic Kelvin-Helmholtz instability. 1. Transverse electrostatic mode," *J. Geophys. Res.*, Vol. 89, 168, 1984.
8. Fujimoto, M. and T. Tetasawa, "Ion inertia effect on the Kelvin-Helmholtz instability," *J. Geophys. Res.*, Vol. 96, 15725, 1991.
9. Pandey, R. S., K. D. Misra, and A. K. Tripathi, "Kelvin-Helmholtz instability in an anisotropic magnetoplasma in the presence of inhomogeneous D.C. electric field parallel flow velocity shear," *Indian J. Radio Space Phys.*, Vol. 30, 113, 2001.
10. Pandey, R. S., K. D. Misra, and A. K. Tripathi, "Generation of ion-cyclotron like wave by parallel flow velocity shear in the presence of inhomogeneous D.C. electric field in an anisotropic magnetoplasma," *Indian J. Radio Space Phys.*, Vol. 32, 75, 2003.
11. Farrugia, C. J., P. E. Sandholt, and L. F. Burlarge, "Auroral activity associated with Kelvin-Helmholtz instability at the inner

edge of the low latitude boundary layer," *J. Geophys. Res.*, Vol. 99, 19403, 1994.

12. Opp, N. and A. B. Hassam, "Kelvin-Helmholtz instability in system with large effective larmor radius," *Phys. Fluid B*, Vol. 3, 885, 1991.
13. Lemons, D. S., D. Winske, and S. P. Gary, "Electrostatic ion-velocity shear instability," *J. Geophys. Res.*, Vol. 97, 19381, 1992.
14. Thomas, V. A. and D. Winske, "Kinetic simulations of the Kelvin-Helmholtz instability at the magnetopause," *J. Geophys. Res.*, Vol. 98, 11425, 1993.
15. Fujimoto, M. and T. Terasawa, "Anomalous ion mixing with in a MHD scale Kelvin-Helmholtz vortex," *J. Geophys. Res.*, Vol. 99, 8601, 1994.
16. Fujimoto, M. and T. Terasawas, "Anomalous ion mixing with in a MHD scale Kelvin-Helmholtz vortex 2. — Effects of in homogeneity," *J. Geophys. Res.*, Vol. 100, 12025, 1995.
17. Mozer, F. S., C. W. Carlson, M. K. Hudson, R. B. Torbert, B. Parady, J. Yatteau, and M. C. Kelley, "Observation of paired electrostatic shocks in the polar magnetosphere," *Phys. Rev. Lett.*, Vol. 38, 292, 1977.
18. Temerin, M., C. Cattell, R. Lysak, M. Hudson, R. Torbert, F. Mozer, R. Sharp, and P. Kintner, "The small scale stucture of electrostatic shocks," *J. Geophys. Res.*, Vol. 86, 11278, 1981.
19. Misra, K. D. and R. S. Pandey, "Generation of Whistler emission by injection of hot electrons in the presence of a.c. electric field in the magnetosphere," *J. Geophysics. Res.*, Vol. 100, 19405, 1995.
20. Pandey, R. S., R. P. Pandey, S. M. Karim, A. K. Srivastava, and Hariom, "The electromagnetic ion-cyclotron instability in the presence of a.c. electric field for Lorentzian kappa," *Progress In Electromagnetics Research M*, Vol. 1, 207, 2008.
21. Huba, J. D., "The Kelvin-Helmholtz instability in inhomogeneous plasma," *J. Geophys. Res.*, Vol. 86, 3653, 1981.
22. Romero, H., G. Ganguli, Y. C. Lee, and P. J. Palmadesso, "Electron-ion hybrid instabilities driven by velocity shear in a magnetized plasma," *Phys. Fluids B*, Vol. 4, 1708, 1992.